Proceedings of the Institute of Acoustics

Modelling DML panels using classical theory

M.R.Avis University of Salford, School of Acoustics and Electronic Engineering
L.D.Copley University of Salford, School of Acoustics and Electronic Engineering

1. INTRODUCTION

Distributed Mode Loudspeaker (DML) panels have been a focus of considerable interest amongst the audio and acoustics community for some time. A number of papers have appeared in recent conference proceedings concerning the design / analysis [eg 1,2] and application [eg 3,4] of these devices; some of these papers have considered the drive mechanism in some detail [5] whilst applying a generalised model for the panel which is sometimes approximated as infinite in extent. Other authors have considered the 'M' in DML rather more explicitly [6], but there remains a considerable body of literature concerning a modal solution for the velocity of finite plates with various boundary conditions, which may be of use in modelling these transducers.

This paper reports the current progress of investigations at Salford whose aim is to apply classical plate theory to the modelling of DML panels, with the intention of gaining insight into the behaviour of the devices and obtaining appropriate physical properties of materials used in their construction.

2. CLASSICAL PLATE THEORY

A useful introduction to the modal behaviour of thin, finite plates is given by Cremer [7]. The approach is clear, but limited in its restriction to simply supported boundary conditions. A more general review of published material (up to 1965) is that of Leissa [8] - the first paper quoted in regard to rectangular plates is that of Warburton [9], and it is with this work that the remainder of this paper is concerned.

Warburton deals with the solution of the familiar fourth-order plate equation for transverse velocity *w*, not only for simply supported but also for free and clamped boundaries.

$$D\nabla^4 w + \rho\frac{\partial^2 w}{\partial t^2} = 0 \qquad where \qquad D = \frac{Eh^3}{12(1-\nu^2)} \tag{1}$$

The solution follows the familiar form of the summation of an infinite number of normal modes, and for point excitation Cremer shows that a damped system may be represented by:

$$w(x,z) = j\omega F\sum_{n=1}^{\infty}\frac{\phi_n(x,z)\,\phi_n(x_0,z_0)}{\Lambda_n\,[\omega_n^2(1+j\eta)-\omega^2]} \tag{2}$$

where:

F =	*force input*	Λ_n =	*normalisation factor*
x_0, y_0 =	*exciter location*	ω_n =	*modal frequency*
x, y =	*receiver location*	ϕ =	*shape function*

So, the spatial distribution of velocity over the surface of the plate is described in terms of modeshapes or eigenvectors, and the resonant frequencies themselves are given by the eigenvalues. Warburton notes that for simply supported boundaries, the eigenvalues and eigenvectors assume the familiar form presented elsewhere by Cremer. Spatial velocity distribution is governed by the summation of a number of sine functions (since the velocity at the plate boundary is zero) and:

$$\phi_n(x,z) = \sin\frac{n_x \pi x}{l_x} \sin\frac{n_z \pi z}{l_z} \tag{3}$$

$$\omega_n = \sqrt{\frac{D}{M}}\left[\left(\frac{n_x \pi}{l_x}\right)^2 \left(\frac{n_z \pi}{l_z}\right)^2\right] \tag{4}$$

Where the boundaries are clamped, or free, both eigenvectors and eigenvalues assume a more complex form. In addition to sine and cos components, spatial velocity distribution requires the inclusion of hyperbolic sinh and cosh terms. Warburton gives expressions for the resonant frequencies associated with such boundary conditions, which together with the appropriate shape functions are reproduced below. Only the result for clamped boundaries is given, since this is the condition used for the practical measurements in this paper. Modeshapes with a dependance on only one spatial coordinate (x) are given - these substitute into **(2)** after multiplication by a similar function with dependance on z.

$$\phi_n(x) = \cos\gamma\left(\frac{x}{l_x} - \frac{1}{2}\right) + k\cosh\gamma\left(\frac{x}{l_x} - \frac{1}{2}\right)$$

$$for\ n_x = 1,3,5... \tag{5a}$$

$$where\ k = \frac{\sin(\gamma/2)}{\sinh(\gamma/2)}\ and\ \tan\gamma/2 + \tanh\gamma/2 = 0$$

$$\phi_n(x) = \sin\gamma'\left(\frac{x}{l_x} - \frac{1}{2}\right) + k'\sinh\gamma'\left(\frac{x}{l_x} - \frac{1}{2}\right)$$

$$for\ n_x = 2,4,6... \tag{5b}$$

$$where\ k' = -\frac{\sin(\gamma'/2)}{\sinh(\gamma'/2)}\ and\ \tan\gamma'/2 - \tanh\gamma'/2 = 0$$

The resonant frequencies are found from

$$\omega_n = \frac{2\lambda h \pi^2}{l_x^2}\left[\frac{E}{48\rho(1-\nu^2)}\right]^{1/2} \tag{6a}$$

where

$$\lambda^2 = G_x^4 + G_z^4\frac{l_x^4}{l_z^4} + \frac{2l_x^2}{l_z^2}\left[\nu H_x H_z + (1-\nu)J_x J_z\right] \tag{6b}$$

and for a plate clamped at all edges

$$n_x = 1: \quad G_x = 1.506\ ,\ H_x = J_x = 1.248 \tag{6c}$$

$$n_x = 2,3,4...:$$

$$G_x = (n_x + 1/2)\ ,\ H_x = J_x = (n_x + 1/2)^2\left[1 - \frac{2}{(n_x + 1/2)\pi}\right] \qquad \textbf{(6c)}$$

with similar expressions in z for the other coordinate axis.

These expressions have been evaluated in terms of transfer impedances as a function of frequency from the excitation point out to some receiver, and in terms of the spatial distribution of velocity over the surface of a plate. These calculations are compared to measurements on physical plates in section 4.

3. MEASUREMENTS ON PRACTICAL PLATES

Leissa notes that whilst theoretical papers on the modal behaviour of plates are numerous, comparisons with measured data are rather harder to obtain. Since the aim of this work is to exploit published theoretical data as a model for a physical DML system, it is important to establish the accuracy of the model. To this end, measurements have been performed on physical plates and compared with the models developed previously.

3.1 Plate excitation and mounting

The derivation of **(2)** requires the evaluation of the surface-integral of the product of input pressure distribution, and the modeshape function ϕ_n:

$$\int_S j\omega p(r)\phi(r)\,dx\,dz \qquad \textbf{(7)}$$

where

r describes location (x,z)

Where the input pressure distribution is simply at one point r_0 having coordinates (x_0, z_0) then the pressure distribution function reduces to a dirac delta function $\delta(r-r_0)$ - then by the 'sifting' property the shape function effectively comes outside the integral as $\phi(r_0)$. The integral then simply produces the factor of area required to change the pressure p of **(7)** to the force F of **(2)**. This makes modelling a *point* force input relatively simple - but means that if other force distributions are to be utilised, the integral **(7)** must first be solved. This problem is analogous to that encountered when considering the excitation of room modes by different shaped sources - Bullmore [11] shows that for rectangular sources a solution is tractable, but the solution for a *ring* distribution as found on most DMLs where the exciter voice coil is glued directly to the panel is not straightforward.

In this paper, point excitation models have been compared with measurements made using an exciter which operates on a very small area (<7e-6 m^2). The practical results might then be expected to de-emphasise modes where the modal bending wavelength approaches the excitation point dimensions , but given its small size this will be a high frequency problem which will not affect low-order panel modes. The model may be extended in future by considering the superposition of a number of point exciters driven in phase, located on the circumference of a ring.

In addition to choosing an appropriate excitation mechanism, it is important to consider the boundary conditions of the panel. Warburton gives data for simply-supported, free and clamped edges (and combinations thereof). Pre-production samples of DML products available at Salford suggest that practical panels may have boundaries secured intermittently or by compliant supports. Leissa suggests methods for the incorporation of these complex boundaries, but in the first instance it was decided to adopt a clamped edge to prove the modelling technique and a suitable measurement rig was constructed.

3.2 Establishing Physical Parameters

A number of physical constants describing the material from which a panel is constructed must be known, in order to implement the model. These include Young's Modulus E, thickness h, Poisson's ratio v, mass/unit area M and loss factor η. The impact of inaccuracies in these coefficients on the final model varies - for instance, error in E has less of an effect than error in η when determining plate velocity, and uncertainty with regard to loss factors can be highly significant [10].

Unfortunately, accurate data concerning panel materials for DML transducers is not always available. In particular, the devices are frequently referred to as 'low-loss' or 'lightly damped' [eg. 5] where inspection suggests this may not always be the case - an assertion which is investigated using these plate models. Of all the parameters mentioned, loss-factor is perhaps least obvious in terms of a measurement method. Cremer notes that it may be extracted from the decay of plate vibrations using the formula:

$$\eta = \frac{2.2}{f.RT_{60}} \tag{7}$$

This requires that the panel be excited at a specific frequency, and the decay time measured when that excitation is removed. A problem with this technique is that the mechanical and electrical damping inherent in the exciter will influence the decay rate of the plate - alternatively time-frequency techniques may be applied where an impulse response is transformed to frequency using overlapping windows and the decay time of various frequency components may be assessed.

Figure 1 shows the impulse response of a 286 x 198 x 0.81mm aluminium plate, clamped at the edges and excited at position (160, 83). A magnetic non-contact pickup was positioned at location (170,60). The aluminium plate was employed since the physical properties of the material are well known, meaning that the modelling technique can be assessed with minimal uncertainty as to the input data. In addition, the aluminum plate is known to be isotropic - for practical DML materials this may not always be the case, and although Leissa makes suggestions for dealing with anisotropy, the evaluation of the technique requires the simplest possible model.

Figure 1 displays a response which is dominated by the decay of the fundamental mode of the plate. A loss-factor may be extrapolated at this frequency with some confidence - in this case

Frequency of fundamental mode = 116Hz   Loss Factor = 2×10^{-2}

3.3 Velocity measurements

DML panels are characteristically constructed using lightweight, stiff materials. Velocity measurements must be carefully contrived so as not to load the panel due to the impedance of the measurement transducer. In the limit, laser velocimetry offers the ultimate non-contact technique [eg 12], but this method has not been available at Salford. Instead, lightweight accelerometers (Knowles BU1771) have been employed; the results obtained have been compared with data collected using non-contact magnetic pickups (eg. Figure 1). No shift in mode frequencies has been observed, suggesting that the mass-load applied by the transducers is insignificant (0.28g). It was necessary to connect the accelerometers using extremely fine enamelled wire, in order to avoid the additional damping imposed by the PVC coating on conventional cable.

The results of practical measurements of plate vibration are displayed in section 4., and are compared to results obtained using the Warburton model of a clamped plate.

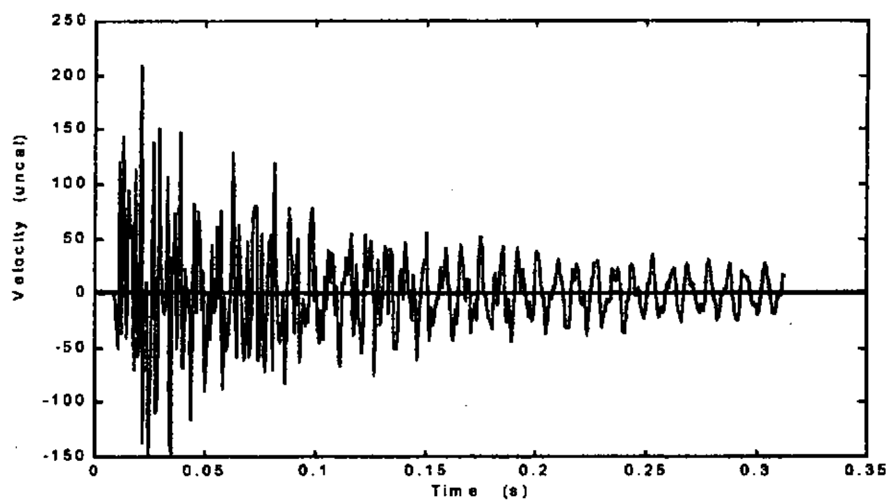

Figure 1 - Measured impulse response of clamped aluminium plate

4. RELATING MEASUREMENTS AND MODELS

4.1 Comparison of Warburton model and measured data

Figure 2 shows a graphical comparison between the Warburton model and a practical measurement on the clamped aluminium plate described in section 3.2. Similar exciter and receiver locations were used - however a moving-coil shaker replaced the force hammer used previously as an exciter. An impedance head allowed the frequency-variation of the force input to be removed from the measurement. Mode orders were verified between model and measurement using two accelerometers to perform a modal survey across the surface of the plate.

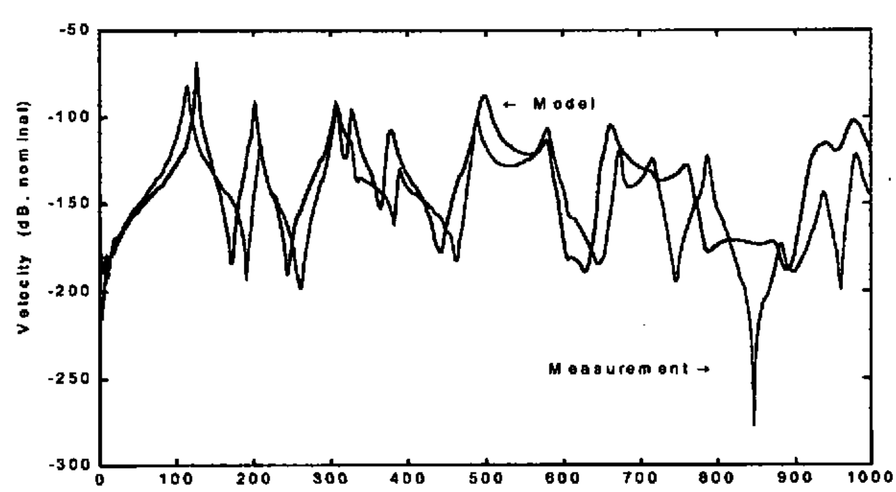

Figure 2 - Measured and modelled frequency response of clamped aluminium plate

A reasonably good match is seen across the displayed bandwidth. As the mass density of the panel was known, 'best-fit' values for Young's modulus and damping factor were obtained by optimising this match. As frequency increases, the model becomes less accurate - perhaps surprisingly, the practical loss-factor appears to decrease as frequency increases.

The radiation impedance presented by the fluid to the plate has been considered. The fluid load has been represented using two simple, idealised models after Beranek [13] and Morse [14]. Both depict the mass loading of an unbaffled, plane circular disk. These have been adapted to accommodate the rectangular plate dimensions using an effective equivalent radius, as a first approximation to the load presented to the fundamental plate mode. In both cases the additional loading did not provide any substantial change to the predicted fundamental resonance, giving less than 0.1% change in terms of the fundamental resonant frequency.

Where a material with a higher loss-factor constitutes the plate material, the fit of the model is rather less satisfactory. Figure 3 shows data for a plate of similar size to that in Figure 2, made of a fibrous hardboard-type material which has been used in production DML panels.

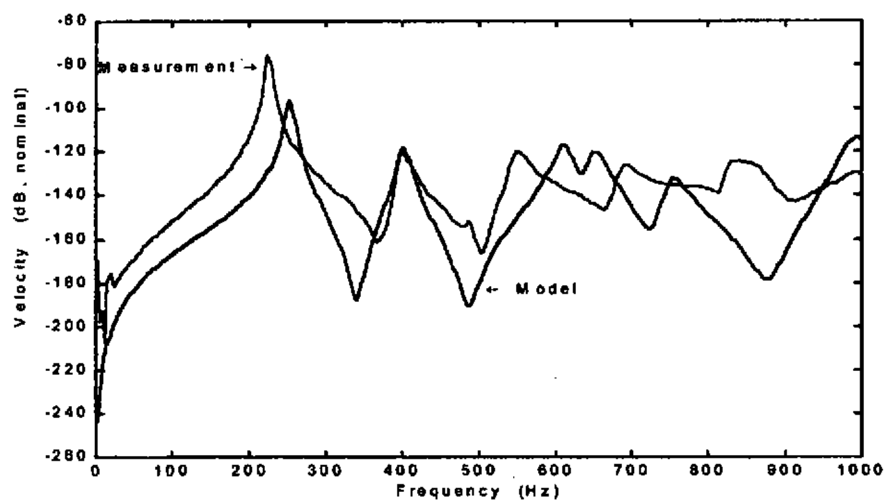

Figure 3 - Measured and modelled frequency response of clamped fibre-board plate

The loss-factor appears to increase with frequency, whereas the model assumes a constant value - a more satisfactory fit would result from an assessment of the damping behaviour of the plate against frequency.

4.2 Spatial velocity distribution and acoustic radiation

As the plate is excited at higher frequencies, and the loss factor increases, modal overlap increases markedly. In terms of the spatial distribution of velocity over the surface of the plate, this has an interesting effect. At lower frequencies where modal overlap is small, one modeshape dominates the summation with the result that point velocities tend to be either in phase or 180° out of phase. At higher frequencies the complex residues of a large number of contributing modeshapes result in a far less 'binary' phase-distribution across the plate surface. In practice, this results in displacement patterns as illustrated in Figure 4.

The exciter location experiences maximal displacement, surrounded by radially-spreading wavefronts which propagate across the surface of the plate. Further away from the exciter there exists a 'reverberant field' of peaks and troughs. (It would not be correct to refer to this region as 'modal' as opposed to a 'direct' contribution from the source - the whole spatial displacement distribution of Figure 4 results from the modal summation of (2), with no explicitly-added direct term.)

This result corresponds closely with acoustic measurements made in terms of the near-field pressure radiated by production DMLs as a function of distance from the excitation point. The maximal

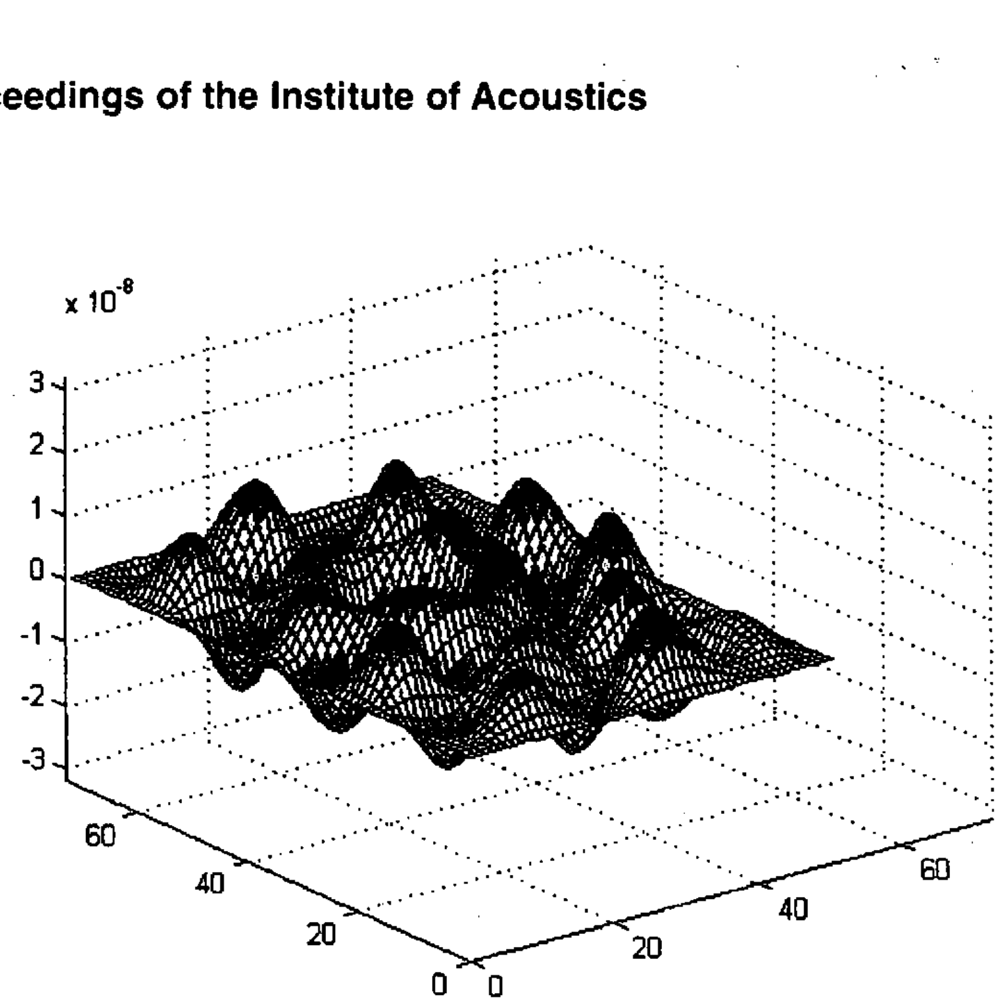

Figure 4 - Modelled displacement of clamped fibre-board plate where f=5 kHz

displacement amplitude found at the exciter corresponds to measurably higher sound pressure levels radiated close to this point. This suggests that rather than a 'chaotic' or 'random' behaviour on the surface of the plate, damping is such that circular wavefronts propagate across the plate surface and predominate the plate radiation. If the damping coefficient were to be much lessened (such as with the aluminium plate) the displacement distribution would become no more random, reverting to the 'binary' phase distribution which results from minimal modal overlap.

This has important ramifications as regards far-field acoustic radiation. It suggests that rather than exhibiting omni-directional behaviour, panels may be highly directional at specific frequencies. Any omnidirectional properties must result from averaging across 1/3 octave (or critical) bandwidths, since depending on plate damping properties the spatial distribution of velocity may change rapidly with excitation frequency [2]. Figure 5 illustrates the modelled directional behaviour of the panel in Figure 4 at a measurement distance of 10m. A large component of high frequency energy is radiated in the plane of the panel, as is experienced in practice - however for angles more towards the normal, a complex pattern of lobes exists due to interference effects between elemental radiators.

5. CONCLUSIONS

These results suggest that classical plate theory can enable the construction of models which are useful in interpreting the vibration and radiation behaviour of DML loudspeakers. It appears that practical DMLs may incorporate reasonably substantial damping which results in high modal overlap. This in turn corresponds to a vibration pattern dominated by the region of the plate close to an exciter, from where circular wavefronts propagate across the plate surface. This would be expected to result in directional behaviour, which is mitigated by changes in the detail of directivity with frequency. Thus when observed using constant percentage rather than narrow band analysis, the devices may show a broad directional characteristic.

Acknowledgements

The authors wish to acknowledge the financial support of the School of Acoustics and Electronic Engineering at Salford, and the contributions of Dr T.J.Cox (Salford) and Dr P.Leclaire (Bradford).

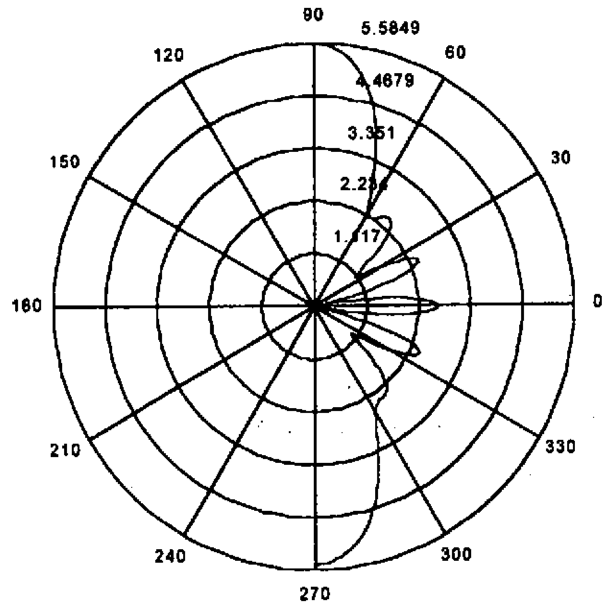

Figure 5 - Modelled polar response (dB) of radiation by clamped fibre-board plate where f=5kHz and r=10m

References

[1] J.Panzer, N.Harris, 'Distributed Mode Loudspeaker Simulation Model', Audio Eng. Soc. 104th Convention, Amsterdam 1998, Preprint 4739

[2] J.A.S.Angus, 'Distributed Mode Loudspeaker Polar Patterns', Audio Eng. Soc. 107th Convention, New York 1999, Preprint 5065

[3] P.Mapp, C.Ellis, 'Improvements in Acoustic Feedback Margin in Sound Reinforcement Systems', Audio Eng. Soc. 106th Convention, Munich 1999, Preprint 4978

[4] H.Azima, J.Panzer, 'Distributed-Mode Loudspeakers (DML) in Small Enclosures', Audio Eng. Soc. 106th Convention, Munich 1999, Preprint 4987

[5] N.Harris, 'A Simple Electro-Mechanical Model of the Distributed-Mode Loudspeaker (DML)', Proc. I.O.A vol.19 part 6, 1997, pp. 59-65

[6] J.Panzer, N.Harris, 'Distributed-Mode Loudspeaker Radiation Simulation', Proc. I.O.A vol.21 part 8, 1999, pp. 57-66

[7] L.Cremer, M.Heckl, E.E.Ungar, 'Structure-Borne Sound', Springer-Verlag Berlin, 1973

[8] A.Leissa, 'Vibration of Plates', Nasa 1973 reprinted Acoust. Soc. Am. 1993

[9] G.B.Warburton, 'The Vibration of Rectangular Plates', Proc. Inst. Mech. Eng. vol. 168 no.12, 1954, pp. 371-384

[10] R.J.M.Craik, 'Statistical Energy Analysis: Theory into Practice', Proc. I.O.A vol.22 part 2, 2000, pp. 1-10

[11] A.J.Bullmore, P.A.Nelson, A.R.D.Curtis, S.J.Elliot, 'The Active Minimisation of Harmonic Enclosed Soundfields 2. A Computer Simulation', JSV 117(1), 1987, pp. 15-33

[12] N.A.Halliwell, 'Laser-Doppler Measurement of Vibrating Surfaces: A Portable Instrument', JSV 62, 1979, pp. 312-315

[13] L.L. Beranek, 'Acoustics', McGraw-Hill, New York 1954 pp. 126

[14] P.M.Morse, K.U.Ingard, 'Theoretical Acoustics', McGraw-Hill, New York 1968 pp. 390